DNDesign: Enhancing Physical Understanding of Protein Inverse Folding Model via Denoising

Youhan Lee
Kakao Brain Corp.
rian.brain@kakaobrain.com

Jaehoon Kim
Kakao Brain Corp.
jack.brain@kakaobrain.com

Abstract

Based on the central dogma that protein structure determines its functionality, an important approach for protein sequence design is to identify promising sequences that fold into pre-designed structures based on domain knowledge. Numerous studies have introduced deep generative model-based inverse-folding, which utilizes various generative models to translate fixed backbones to corresponding sequences. In this work, we reveal that denoising training enables models to deeply capture the protein energy landscape, which previous models do not fully leverage. Based on this, we propose a novel Denoising-enhanced protein fixed backbone design (DNDesign), which combines conventional inverse-folding networks with a novel plug-in module, which learns the physical understanding via denoising training and transfers the knowledge to the entire network. Through extensive experiments, we demonstrate that DNDesign can easily be integrated into state-of-the-art models and improve performance in multiple modes, including auto-regressive, non-auto-regressive, and scaled-up scenarios. Furthermore, we introduce a fixed backbone conservation analysis based on potential energy changes, which confirms that DNDesign ensures more energetically favorable inverse-folding.

1 Introduction

Proteins play a crucial role in various biological processes, serving as the primary components of cellular machinery and exhibiting specific functionalities based on their three-dimensional structures. Therefore, designing unique protein sequences that fold into the pre-designed structures to have targeted functionality is of great importance in various biological applications, including pharmaceuticals, biofuels, biosensors, and agriculture [1, 2, 3, 4, 5]. Mutagenesis aided with high-throughput experiments and physics-based computational methods have been proposed to address this problem in the past [6, 7].

Recently, a new paradigm employing a deep generative model conditioning on three-dimensional structures has gained attention, and its results have been encouraging. These models typically represent a given fixed protein backbone as a 3D graph and leverage advanced generation techniques such as auto-regressive, non-auto-regressive, or adapter-based methods to translate fixed protein backbones into corresponding sequences that can achieve specific biological purposes [8]. For example, Daurass et al. [9] experimentally proved that the deep inverse folding neural networks(IFNN) generates protein sequences with targeted functionality at a higher success rate than Rosetta, a well-established software widely used in the protein community.

As the folding structure is a consequence of the physics that causes folding, acquiring meaningful physical knowledge of folding structures, called folding energy landscape, directly from data would benefit generative models. The currently proposed DIFM has utilized geometric-related features and geometric neural networks to maximize the likelihood of the given training data, aiming to comprehend the protein world and perform inverse-folding based on the physical understanding.

Preprint. Under review.

However, the experimentally validated structural data is limited to about 200K [10], and the number of structurally distinct and unique proteins practically used for inverse-folding training is only around 30K [11], which is insufficient to train a model to grasp the nature of complex protein folding systems fully. In addition, considering de novo proteins with significantly different characteristics from those discovered thus far, the data scarcity problem worsens more.

In this study, we present DNDesign, a DeNoising-enhanced protein DESIGN framework, which maximizes the model's physical understanding directly from training data. First, we prove that denoising training directly on a three-dimensional backbone structure is equivalent to the direction of energy minimization, finally enabling the models to learn the folding energy landscape. Then, we suggest a novel folding physics learning plug-in module (FPLM), which can be integrated into existing inverse-folding neural networks. First, IFNN takes the original structure, while FPLM inputs the perturbed structures obtained by adding noises to the original structure. Then, FPLM learns the folding energy landscape by moving the perturbed structure to the energetically stable state. To effectively transfer the folding knowledge to IFNN, FPLM employs five novel operations: (1) force feature initialization, (2) force-node attention, (3) force-edge attention, (4) global force attention, and (5) force biasing to transfer the physical inductive bias to the entire network. Notably, the force biasing operation allows the sequence decoder to conduct sampling while considering folding physics. Finally, DNDesign enables IFNN to learn four pieces of information, including original structure, intermediate structure, folding physics, and the direction of energy minimization using given data, enhancing previous methods which only know the original structure.

To demonstrate the novelty of DNDesign, we conduct a series of protein sequence design tasks. Particularly, to showcase the "easy-to-use" nature and generalization of DNDesign, we apply DNDesign to three representative IFNN settings, including auto-regressive (AR), non-auto-regressive (NAR), and scaled-up settings. Remarkably, DNDesign consistently improves the previous method in all experiments, proving that more physical understanding from denoising training benefits models to conduct successful inverse-folding. In addition to considering sequence consistency estimated using the sequence recovery metric, we evaluate the structure conservation by measuring the potential energy change caused by generated sequences after structure relaxation. Based on this metric, we have demonstrated that DNDesign enables models to generate more energetically favorable sequences. To our knowledge, this is the first work comparing structure conservation using potential energy change for evaluating deep inveres-folding models. In addition, extensive ablation and analysis are provided to help the understanding of DNDesign. Our contributions are as follows:

- We propose DNDesign, which enables the inverse-folding model to capture the deep understanding of folding physics that previous models do not fully exploit.
- We prove how DNDesign learns folding physics directly from data and show that DNDesign improves the state-of-the-art model on various protein sequence design benchmarks in auto-regressive, non-auto-regressive, and scaled-up scenarios.
- We introduce a fixed backbone conservation task based on potential energy change from newly generated sequences. The analysis proves that DNDesign generates energetically favorable sequences, leading to more fine-grained protein design.

2 Preliminaries and Related works

2.1 Protein representation

A protein is a sequence $P = \{A_1, ..., A_N\}$ where A_i is a residue of 20 types of amino acids. Each amino acid is composed of backbone atoms including C, N, C_α, O and side chain R_i consisting of atoms, which determine the property of the amino acid, and each atom has coordinate $\mathbf{x} \in \mathbb{R}^3$. Following ingraham et al [12], each residue has geometry derived from backbone atoms, called local coordinate system $g_i = [b_i, n_i, b_i \times n_i]$, where,

$$u_i = \frac{\mathbf{x}_{C_{\alpha i}} - \mathbf{x}_{N_i}}{\|\mathbf{x}_{C_{\alpha i}} - \mathbf{x}_{N_i}\|}, v_i = \frac{\mathbf{x}_{C_i} - \mathbf{x}_{C_{\alpha i}}}{\|\mathbf{x}_{C_i} - \mathbf{x}_{C_{\alpha i}}\|}, b_i = \frac{u_i - v_i}{\|u_i - v_i\|}. \tag{1}$$

Because each side-chain corresponds to each amino acid residue s, a protein can be represented as a sequence of residue and geometry pairs, $P = \{(s_i, g_1), ..., (s_N, g_N)\}$ as depicted in Figure 1.

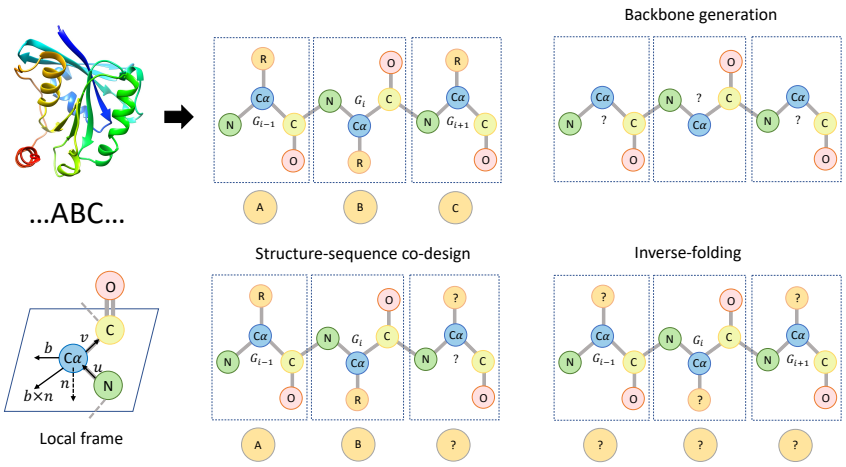

Figure 1: Overview of protein representation and types of structure-based protein design.

2.2 Structure-based Protein Design

Because we can reconstruct side-chain R using both backbone G and residues S, structure-based protein design only focuses on the generation of backbone G and residues S. Neural structure-based protein design can be categorized into three tasks, (1) backbone generation, (2) structure-sequence co-design, and (3) inverse-folding depending on design scenarios as illustrated in Figure 1.

Backbone generation Backbone generation can be formulated as an end-to-end structure-to-structure generation as $f_\theta : G \rightarrow G$. We train parameterized encoder-decoder neural networks f_θ to sample diverse and plausible backbone structures. We note that this approach requires a model which can assign amino acids are required to obtain complete proteins [13].

Structure-sequence co-design The structure-sequence co-design approach generates sequences and backbone structures simultaneously as $f_\theta : (G, S) \rightarrow (G, S)$. By generating sequences autoregressively and refining predicted structures iteratively, this co-design approach enables the adaptive generation of optimized sequences compatible with the flexible backbone. This approach is suitable for scenarios such as antibody design, where global structure tends to be changed depending on the designed antibody [14].

Inverse-folding Inverse-folding is an approach that aims to "caption" or "translate" a provided backbone structure into potential protein sequences as $f_\theta : G \rightarrow S$. Inverse-folding becomes particularly valuable for protein functional design problems, such as ligand binding site, enzyme, and binder design, which require fine-grained control over side-chain combinations. Since there exist numerous sequences that can fold into a specific backbone conformation [15], inverse-folding approach enables protein engineers to identify diverse and promising protein sequences with optimized functional properties [1, 2, 3, 4, 5].

2.3 Importance of physical understanding for structure-based protein design

The folding structure of proteins is governed by the physics that determines the folding process. Therefore, a higher level of understanding of physics enables a model to perform well in structure-related tasks. For instance, AlphaFold2 [16] achieved nearly experimental-level accuracy in structure prediction and has revolutionized protein fields since its publication. Recently, [17] proved that the success of AlphaFold2 [18] is attributed to the data-driven understanding of the folding energy landscape. Additionally, RFDiffusion [13] demonstrated that physically plausible and synthesizable structures were created when generative models were trained upon pre-trained protein structures model, especially, RoseTTAFold [18] that comprehend the mechanism of folding. On the other hand, RefineDiff [19] showed that physics learning enhances protein representation learning for various downstream tasks.

3 Related works

3.1 Deep generative protein design

Deep generative models for protein design can be classified into four categories: sequence-to-sequence, structure-to-structure, structure-to-sequence, and structure-sequence co-design. In the sequence-to-sequence category, several notable works, such as RITA [20], DARK [21], ProtGPT2 [22], and ProGen2 [23] have applied language modeling techniques to analyze large protein sequence databases and successfully generated novel protein sequences. Moving on to the structure-to-structure category, deep generative models, such as variational autoencoders [24], generative adversarial networks [25], or diffusion models [26, 27], have been applied to this problem and shown promising results for generating diverse and structurally plausible protein backbones [28, 29, 13, 30, 31, 32]. Third, in the structure-to-sequence category, deep generative inverse-folding models, such as GraphTrans, GVP, ProteinMPNN, PiFold [12, 33, 34, 35, 36, 9] have been proposed. These models predict or generate protein sequences corresponding to a given protein backbone structure, allowing for the design of functional proteins with specific structural constraints. Last, DiffAb [37] and RefineGNN [38] generate structure and sequence simultaneously through iterative refinement. Our proposed DNDesign falls within the category of deep generative inverse-folding models. DNDesign differentiates itself from previous approaches by utilizing denoising to strengthen the understanding of models.

3.2 Denoising training for chemical and biology system modeling

In order to effectively model chemical and biological systems, acquiring meaningful physical knowledge directly from data plays a crucial role in successful representation learning and downstream tasks. Over the past decade, numerous studies have proposed novel deep learning architectures and training methods that demonstrate remarkable performance in approximating interactions and quantum properties [39, 40, 41, 36, 42]. Recently, several works have theoretically established the equivalence between denoising training on biological molecule data and learning the underlying physical force field [43, 44, 19]. Building upon this finding, Godwin et al. [45] successfully addressed the over-smoothing challenge in graph neural networks (GNNs) by employing denoising training on three-dimensional coordinates as an auxiliary loss. Their approach achieved state-of-the-art results on various quantum chemistry downstream tasks. Similarly, [43] utilized denoising as a pre-training objective on the 3M molecular dataset and demonstrated that denoising-based learning produces high-quality representations based on a data-driven force field, effectively solving different molecular benchmarks. In this work, we adopt a similar denoising-based approach to that of [45, 19]. Our work is similar to [19], which utilized denoising to learn folding physics, but they focused on representation learning. Otherwise, our work first extend denoising to protein sequence generation. Despite this difference, the inductive bias gained from DNDesign is identical to that of the two aforementioned papers.

4 Methods

4.1 Overview

DEDesign integrates conventional inverse-folding networks (IFNN) with denoising networks (FPLM). In this section, we begin by elucidating the process of protein featurization. Subsequently, Section 4.3 outlines the model architecture and describes the feature update operation in IFNN. Next, section 4.4 highlights the correlation between the denoising process and the acquisition of folding physics knowledge. Finally, Section 4.5 describes the five operations utilized to transfer data-driven folding physics across the entire network.

4.2 Featurization

In this work, we regard a protein as a k-NN 3D graph $G(V, E, X)$, where V, E, X are node features, edge features, and xyz coordinates, respectively. As suggested in [12], node and edge features are constructed considering pairwise distances, angle, torsion, and directions using the four backbone atoms of each node. Each node and edge feature is input to a single fully-connected layer and converted into an embedding vector, h^0, e^0, respectively. More details are illustrated in Appendix A.

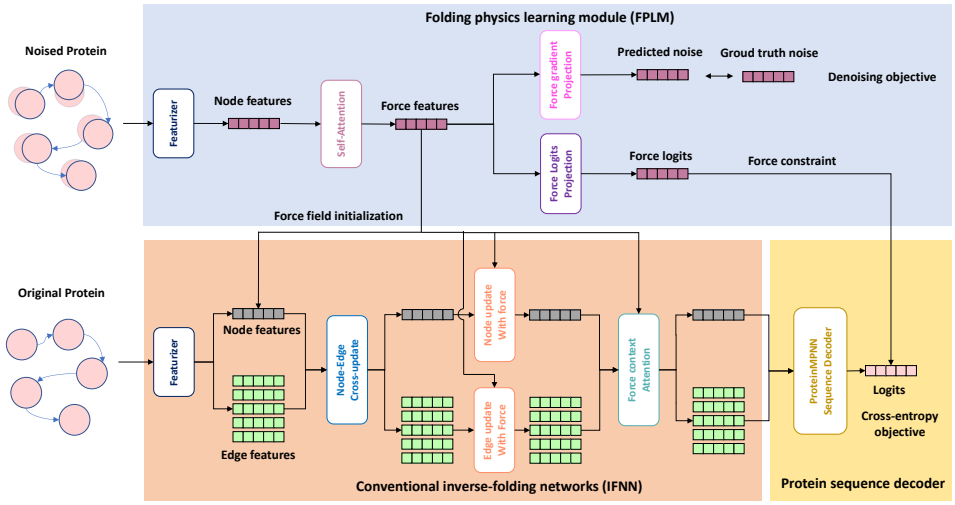

Figure 2: Overview of the proposed DNDesign.

4.3 Conventional inverse-folding model modeling

In this subsection, we will briefly describe the IFNN used in this work. As shown in Figure 2, we adopt a state-of-the-art inverse-folding encoder, called PiGNN proposed by [46]. We first update node and edge features in order based on k-NN neighbors. And, the node features h_i^l and edge features e_i^l are obtained using a featurizer and updated using a simplified graph transformer [47]. After computing the node value using the edge features and neighbor node features, we multiply the softmax values of the attention weights obtained from h_i^l and e_i^l to the node value and add the weights to the node features. Finally, we update the h_i^l to obtain the next layer node features h_i^l using a learnable weight function with normalization and residual connection. Edge features e_{ji}^l are calculated by passing concatenation of node feature h_i, neighbor node feature h_j, and edge feature $e_{i,j}$ to the MLP ψ^e.

We use two types of inverse folding decoders to predict logits: (1) auto-regressive (AR) and (2) non-auto-regressive (NAR). For AR, we employ the sequence decoder used in GraphTrans [12] and utilize random decoding introduced by ProteinMPNN [9]. For NAR, we use a linear layer as [33]. The decoder inputs node feature h_j and outputs logits. The whole IFNN is trained by minimizing the negative log-likelihood $\mathcal{L}_{AR}$ of the data.

4.4 Folding physics learning via denoising

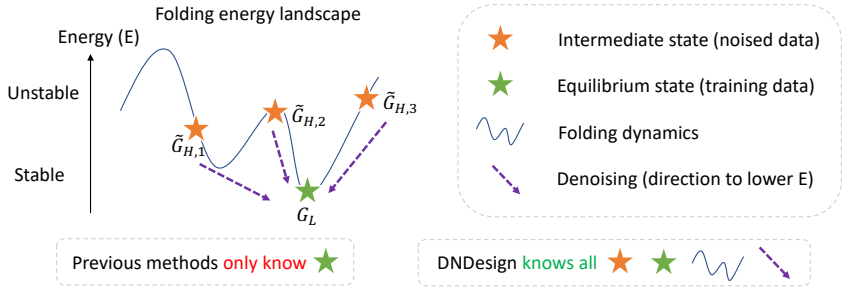

Figure 3: Illustration of Energy landscape of protein folding. DNDesign enable inverse-folding model to capture all information of folding physics.

Folding energy landscape The protein structure $G = \{g_1, ..., g_N\}$ that a protein P with sequence $S = \{s_1, ..., s_N\}$ can have is diverse, and each structure corresponds to a specific potential energy E

based on the folding physics, represented as the folding energy landscape. Considering the dynamics that structure prefers energetically stable states, each protein structure G used in training data can be regarded as the most stable, i.e., energetically lowest structure G_L among the various folding states that each sequence can possess.

Figure 3 illustrates four crucial pieces of information contained within the energy landscape: (1) stable or low energy state G_L, (2) unstable or high energy state $\tilde{G}_H$, (3) folding physics, i.g, energy potential, and (4) the direction or gradient ∇G that transforms the unstable state $\tilde{G}_H$ to the stable state G_L.

Perturbation on backbone structure Firstly, since we only have G_L in the training data, we obtain $\tilde{G}_H$ by adding Gaussian noise to G_L. G is a sequence of local frames g, where each g consists of a C_α coordinate vector, $\mathbf{x}$, and an $SO3$ vector, $\mathbf{r}$. To account for this nature, we follow the forward noising procedure used in [48, 37]. For x, we use random three-dimensional Gaussian noise, which can be described as follows:

$$q\left(\mathbf{x}_j^T \mid \mathbf{x}_j^{T-1}\right) = \mathcal{N}\left(\mathbf{x}_j^T \mid \sqrt{1-\beta_{pos}^T} \cdot \mathbf{x}_j^{T-1}, \beta_{pos}^T \mathbf{I}\right). \tag{2}$$

$$q\left(\mathbf{x}_j^T \mid \mathbf{x}_j^0\right) = \mathcal{N}\left(\mathbf{x}_j^T \mid \sqrt{\bar{\alpha}_{pos}^0} \cdot \mathbf{x}_j^0, (1-\bar{\alpha}_{pos}^0)\mathbf{I}\right). \tag{3}$$

where N denotes a Gaussian distribution.

For perturbing r, we use an isotropic Gaussian distribution with a mean rotation scalar variance parameter in the SO3 space [48, 49, 50] as follow:

$$q\left(\mathbf{r}_j^T \mid \mathbf{r}_j^0\right) = \mathcal{IG}_{SO(3)}\left(\mathbf{r}_j^T \mid \lambda(\sqrt{\bar{\alpha}_{ori}^T}, \mathbf{r}_j^0), 1-\bar{\alpha}_{ori}^T)\right) \tag{4}$$

, where λ is a modification of the rotation matrix by scaling its rotation angle with the rotation axis fixed [51].

Denoising training Based on the remarkable reparameterization technique proposed by Ho et al. [26] and definition of training objective [37], we can optimize denoising objectives for the transition vector t and $SO3$ vector r as follows:

$$L_{pos}^t = \mathbb{E}\left[\frac{1}{M}\sum_j \|\epsilon_j - \psi(\tilde{G}_H, t)\|^2\right],\ L_{ori}^t = \mathbb{E}\left[\frac{1}{M}\sum_j \|(r_j^0)^{\mathbf{T}}\psi(\tilde{G}_H, t) - \mathbf{I}\|_F^2\right] \tag{5}$$

, where ψ is a neural networks that predicts the perturbation on t and r. L_{pos}^t is mean squared error between added Gaussian noise ϵ_j and predicted noises $\psi(\tilde{G}_H, t)$ and L_{rot}^t minimizes the discrepancy calculated by the inner product between the real and predicted orientation $\psi(\tilde{G}_H, t)$.

Learning folding physics through denoising learning From a statistical perspective, denoising training can be seen as learning the Boltzmann distribution $p_{physical}(G)$, which represents the probability distribution $p_{physical}(G) \propto \exp(-E(G))$ of the structure's energy E using a given protein structure G as a random quantity. Based on the definition, the derivative $\nabla_{\mathbf{x}} \log p_{physical}$ of the folding energy potential $E(G)$ corresponds to the force $-\nabla_{\mathbf{x}} E(\mathbf{x})$ acting on the backbone atoms, directing them towards energetically stable directions as follows:

$$\nabla_{\mathbf{x}} \log p_{physical} = -\nabla_{\mathbf{x}} E(\mathbf{x}) \tag{6}$$

Since $p_{physical}$ is unavailable in practice, we approximate it using data. Following [52], we can compute the log-likelihood of p_0 using

$$\log p_0(X(0)) = \log p_T(x(T)) + \int_0^T \nabla \cdot \tilde{f}_\sigma(x(t), t)dt. \tag{7}$$

So, we can approximate p by approximating $\tilde{f}$. To do that, we use Gaussian noise $q_\sigma(\tilde{G}_H^T \mid G_L) = \mathcal{N}(\tilde{G}_H^T; G_L, \sigma^2\mathcal{I}_{3N})$ as used in other works [27, 26], then, we finally can match the score $\nabla_{\mathbf{x}} \log p_{physical}$ by learning neural networks $\theta(\tilde{G}_H^T, T)$ that predict $\nabla_{\tilde{\mathbf{x}}} \log q_\sigma(\tilde{G}_H^T \mid G_L)$.

$$E_{q_\sigma(\tilde{G}_H^T \mid G_L)}\left[\|\theta(\tilde{G}_H^T, T) - \nabla_{\tilde{\mathbf{x}}} \log q_\sigma(\tilde{G}_H^T \mid G_L)\|^2\right] \tag{8}$$

This score-matching is the same as what we use in the DNDesign framework. So, we can conclude that denoising $\tilde{G}_H$, which has become a higher energy state due to noise, towards G_L is equivalent to learning the folding dynamics.

In summary, in DNDesign, we employ denoising training to learn the energy potential that determines the folding state, i.e., the folding energy landscape. Finally, unlike all previous methods that only train for (1), DNDesign allows for the training of (1), (2), (3), and (4) simultaneously, maximizing the model's physical understanding within the given data.

4.5 Physics understanding transfer

This section describes FPLM and the five operations to transfer the folding physics inductive bias of DENN to IFNN.

Feature embedding We first extract geometric features of perturbed structure and update the features using orientation-aware roto-translation invariant network networks used in [37]. We call the features force features and use the features in the following five operations.

Node initialization with force We add force features to the initial node features so that all node and edge features update in IFNN can be conducted using folding physics understanding.

$$h_i^0 = h_i^0 + f_i^{l+1} \tag{9}$$

Node update with force For node updates using force features, we use an attention module that combines two operations: self-attention and cross-attention. The two attentions are based on multi-headed full self-attention [53]. First, self-attention on node features is conducted. Then, cross-attention is performed between the self-attended node features and the force features. At this time, the query and key are force features, and through this, each node strongly interacts with the force state of all other nodes.

Edge update with force Edge updates with force features are performed similarly to edge updates with node features in IFNN. After concatenating the force feature f_i, the force feature of the neighbor j node f_j, and the edge features e_{ij} corresponding to the ij pair, edge feature e_{ji}^l is obtained by projecting the concatenated features into the learnable MLP ψ^f.

$$e_{ji}^l = \psi^f(f_j^{l+1} \| e_{ji,1}^l \| f_i^{l+1}) \tag{10}$$

Global force context attention The global force state summing all local forces is an essential context for protein sequences. In the above two modules, node and edge updates are conducted using local forces. As the last module, we update node and edge features using the global force state features. The total global force state is simply calculated by taking the average of all force state features. To reduce computational costs, we apply an element-wise product using gated attention combined with a sigmoid function to each node and edge. By doing so, the global force information is transferred to all nodes and edges that comprise a protein.

$$f_i = Mean(\{f_k^{l+1}\}_{k \in \mathcal{B}_i}) \tag{11}$$

$$h_i^{l+1} = h_i^l \odot \sigma(\phi^n(f_i)) \tag{12}$$

$$e_{ji}^{l+1} = e_{ji}^l \odot \sigma(\phi^e(f_i)) \tag{13}$$

Sequence sampling with end-to-end physics constraint We obtained logits using force features through linear layer and add the logits to the logits of IFNN as follow:

$$l = \alpha l_s + (1 - \alpha) l_f \tag{14}$$

The ratio of force to decoder logits is empirically determined. In this work, we use 0.2 of α. By different ratios, we can generate diverse sequences by conditioning on physics features. This adds an additional sampling parameter to inverse-folding sampling, which only resort to probability-based sequence sampling previously.

Table 1: Protein sequence design comparison on CATH 4.2 in both AR and NAR settings. † indicates scores copied from [33], and ‡ indicates the newly calculated scores in our setting.

Model	Type	Perplexity ↓			Recovery % ↑		
		Short	Single-chain	All	Short	Single-chain	All
StructGNN†	AR	8.29	8.74	6.40	29.44	28.26	35.91
GraphTrans†		8.39	8.83	6.63	28.14	28.46	35.82
GVP†		7.23	7.84	5.36	30.60	28.95	39.47
ProteinMPNN†		6.21	6.68	4.61	36.35	34.43	45.96
PiFold‡		6.31±0.03	6.73±0.08	4.63±0.01	38.50±0.56	36.31±0.54	48.91±0.28
DNDesign-PiFold‡		**5.70**±0.09	**6.03**±0.08	**4.49**±0.02	**39.09**±0.46	**36.83**±0.49	**49.88**±0.29
PiFold‡	NAR	6.75±0.03	7.21±0.10	5.05±0.04	39.93±0.10	37.88±0.52	49.49±0.16
DNDesign-PiFold‡		**6.72**±0.17	**7.07**±0.25	**4.96**±0.04	**40.18**±0.74	**38.65**±1.46	**49.93**±0.42

Table 2: Protein sequence design comparison on CATH 4.3 in the scaled-up setting. † indicates scores copied from [8], and ‡ indicates the newly calculated scores in our setting.

Model	Type	Perplexity All	Recovery % ↑ All
GVP-GNN†	AR	6.06	38.20
GVP-Large†	AR	4.08	50.80
GVP-transformer-Large†	AR	4.01	51.60
PiFold‡	AR	3.97±0.01	52.06±0.08
DNDesign-PiFold‡	AR	**3.80**±0.01	**53.75**±0.25

5 Experiments

In this section, we compare FFDesign with the state-of-the-art deep generative inverse-folding models in three scenarios, including single-chain, multi-chain, and real-world datasets.

5.1 Experiment Setting

Implementation details We choose PiFold as IFNN and train PiFold and DNDesign-PiFold in AR, NAR, and scaled-up settings. Models are trained up to 100 in AR and NAR settings, and we set 150 epochs for the scaled-up scenario. All models are trained on 1 NVIDIA A100s with the Adam optimizer [54]. The batch size contains 6000 tokens, and the learning rate is set to 0.001 and decayed with OneCycle scheduler. More details are provided in the appendix. For reliable experiments, all results are obtained using three seeds.

Baselines We employ various graph-based inverse-folding models as baselines, including StructGNN, StructTrans [12], GCA [55], GVP [34], GVP-large [8], GVP-transformer [8], AlphaDesign [47], ESM-IF [8], ProteinMPNN [9], and PiFold [33].

5.2 Main Results

Single-chain sequence design CATH [11] is a widely used protein dataset to evaluate inverse-folding models on single-chain sequence design tasks. For a fair comparison, we adopt the version of CATH4.2 as used in GraphTrans and GVP, PiFold. In CATH 4.2, 18024, 608, and 1120 proteins are used for training, validation, and testing, respectively. In the standard setting for this task, models are trained using training data and evaluated on three sets from the test set; short-chain, single-chain, and all-set, with perplexity and median recovery scores. Sequence recovery is a widely used metric for inverse-folding and measures how many residues of sampled sequences match that of the ground truth sequence at each position. The results on CATH 4.2 are shown in Table 1. Under similar conditions, the proposed DNDesign consistently improves the previous SOTA method on both perplexity and recovery in both auto-regressive and non-auto-regressive settings.

Scaling-up [8] proved that additional structure data predicted using AlphaFold2 gives remarkable improvement for sequence design. Likewise, we prepare ∼12M predicted structure data of Uniref50 [56] from AlphaFold2 database and train both PiFold and DNDesign-PiFold models using CATH 4.3 + Uniref50. Interestingly, the improvement from denoising becomes more evident in a scaled setting, as shown in Table 2. These results indicate that even with scaling up by adding

millions of structures, a model still accesses only the given stable structures. However, models trained using DNDesign can fully leverage all four pieces of information in folding physics, resulting in improved performance.

Other benchmarks We also conduct sequence design on multi-chain and real-world datasets, TS50, TS500 [57], and Ollikainen [58] datasets. As shown in Appendix A, performance gains from denoising still appear, proving the importance of folding physics understanding for protein inverse-folding design. Detailed results are provided in the appendix.

5.3 Analysis

In this section, we provide analyses to understand DNDesign more deeply. This section includes fixed backbone conservation using potential energy and an ablation study about five proposed operations. Additional analyses, such as core-surface analysis and other ablation studies, are provided appendix.

Fixed backbone conservation study Sequence recovery is suitable for measuring sequence consistency, but it cannot fully describe the potential energy behavior. In fixed backbone design, the ultimate goal is to generate sequences with the given structure. Therefore, it is necessary to evaluate whether the generated sequences conserve the fixed backbone structure. Conservation of the given structure implies that the generated sequences pose a structure that do not deviate far from the minimum energy state of the structure. Thus, we can evaluate whether the model generates energetically stable sequences by performing structure relaxation on the sampled proteins, which have corresponding new sequences and given backbone, and measuring the potential energy change. We utilize the Rosetta [59], a well-published computational tool, for structure relaxation. We use 282 structures after filtering structures having residues without coordinates. We generated nine sequences for each structure and performed relaxation for each (structure, sequence) pair. Then, we computed the change of potential energies. Interestingly, as shown in Figure 4, we observe that PiFold, with an enhanced understanding of folding physics from DNDesign, generates more sequences with potential energy change near zero, meaning complete structure conservation. This clearly demonstrates that our approach, which emphasizes the importance of physics in fixed backbone design and addresses it through denoising, works. To the best of our knowledge, this is the first work comparing fixed backbone conservation using potential energy in fixed backbone design.

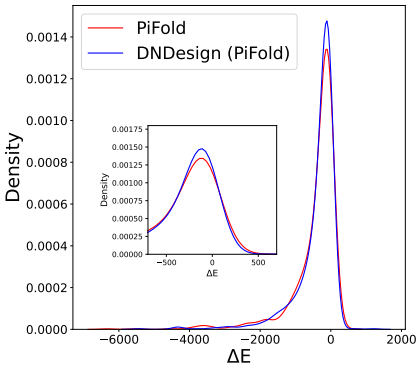

Figure 4: Distribution of potential energy change of structures caused by generated sequences.

Ablation study To understand the effectiveness of each additional force field supervision, we conduct an ablation study, as shown in Appendix B. All components show improvement over baseline, meaning that the folding physics inductive bias is effectively transferred to the entire networks.

6 Conclusion

In this study, we have demonstrated that denoising can learn folding physics, and based on this insight, we proposed the DNDesign framework. The proposed framework can easily be integrated into existing SOTA models and has shown performance improvements in various sequence design tasks across multiple settings. Particularly, we evaluated the impact of the acquired energy potential knowledge from the proposed framework by directly assessing its influence on potential energy through the fixed backbone conservation task. This evaluation provides evidence that the model trained with denoising generate energetically favorable sequences. This work sheds light on the significance of learning physics in structure-based protein sequence design, both theoretically and experimentally, and provides energy-based evidence. We hope that our work inspires future research in the structure-based design protein field.

References

[1] Daniela Röthlisberger, Olga Khersonsky, Andrew M Wollacott, Lin Jiang, Jason DeChancie, Jamie Betker, Jasmine L Gallaher, Eric A Althoff, Alexandre Zanghellini, Orly Dym, et al. Kemp elimination catalysts by computational enzyme design. *Nature*, 453(7192):190–195, 2008.

[2] Justin B Siegel, Alexandre Zanghellini, Helena M Lovick, Gert Kiss, Abigail R Lambert, Jennifer L St. Clair, Jasmine L Gallaher, Donald Hilvert, Michael H Gelb, Barry L Stoddard, et al. Computational design of an enzyme catalyst for a stereoselective bimolecular diels-alder reaction. *Science*, 329(5989):309–313, 2010.

[3] Scott E Boyken, Zibo Chen, Benjamin Groves, Robert A Langan, Gustav Oberdorfer, Alex Ford, Jason M Gilmore, Chunfu Xu, Frank DiMaio, Jose Henrique Pereira, et al. De novo design of protein homo-oligomers with modular hydrogen-bond network–mediated specificity. *Science*, 352(6286):680–687, 2016.

[4] Nathan H Joh, Tuo Wang, Manasi P Bhate, Rudresh Acharya, Yibing Wu, Michael Grabe, Mei Hong, Gevorg Grigoryan, and William F DeGrado. De novo design of a transmembrane zn2+-transporting four-helix bundle. *Science*, 346(6216):1520–1524, 2014.

[5] Gevorg Grigoryan, Yong Ho Kim, Rudresh Acharya, Kevin Axelrod, Rishabh M Jain, Lauren Willis, Marija Drndic, James M Kikkawa, and William F DeGrado. Computational design of virus-like protein assemblies on carbon nanotube surfaces. *Science*, 332(6033):1071–1076, 2011.

[6] Bassil I Dahiyat and Stephen L Mayo. Probing the role of packing specificity in protein design. *Proceedings of the National Academy of Sciences*, 94(19):10172–10177, 1997.

[7] Arthur G Street and Stephen L Mayo. Computational protein design. *Structure*, 7(5):R105–R109, 1999.

[8] Chloe Hsu, Robert Verkuil, Jason Liu, Zeming Lin, Brian Hie, Tom Sercu, Adam Lerer, and Alexander Rives. Learning inverse folding from millions of predicted structures. In *International Conference on Machine Learning*, pages 8946–8970. PMLR, 2022.

[9] Justas Dauparas, Ivan Anishchenko, Nathaniel Bennett, Hua Bai, Robert J Ragotte, Lukas F Milles, Basile IM Wicky, Alexis Courbet, Rob J de Haas, Neville Bethel, et al. Robust deep learning–based protein sequence design using proteinmpnn. *Science*, 378(6615):49–56, 2022.

[10] Joel L Sussman, Dawei Lin, Jiansheng Jiang, Nancy O Manning, Jaime Prilusky, Otto Ritter, and Enrique E Abola. Protein data bank (pdb): database of three-dimensional structural information of biological macromolecules. *Acta Crystallographica Section D: Biological Crystallography*, 54(6):1078–1084, 1998.

[11] Christine A Orengo, Alex D Michie, Susan Jones, David T Jones, Mark B Swindells, and Janet M Thornton. Cath–a hierarchic classification of protein domain structures. *Structure*, 5(8):1093–1109, 1997.

[12] John Ingraham, Vikas Garg, Regina Barzilay, and Tommi Jaakkola. Generative models for graph-based protein design. *Advances in neural information processing systems*, 32, 2019.

[13] Joseph L Watson, David Juergens, Nathaniel R Bennett, Brian L Trippe, Jason Yim, Helen E Eisenach, Woody Ahern, Andrew J Borst, Robert J Ragotte, Lukas F Milles, et al. Broadly applicable and accurate protein design by integrating structure prediction networks and diffusion generative models. *bioRxiv*, 2022.

[14] Matthew IJ Raybould, Claire Marks, Konrad Krawczyk, Bruck Taddese, Jaroslaw Nowak, Alan P Lewis, Alexander Bujotzek, Jiye Shi, and Charlotte M Deane. Five computational developability guidelines for therapeutic antibody profiling. *Proceedings of the National Academy of Sciences*, 116(10):4025–4030, 2019.

[15] William R Pearson and Michael L Sierk. The limits of protein sequence comparison? *Current opinion in structural biology*, 15(3):254–260, 2005.

[16] John Jumper, Richard Evans, Alexander Pritzel, Tim Green, Michael Figurnov, Olaf Ronneberger, Kathryn Tunyasuvunakool, Russ Bates, Augustin Žídek, Anna Potapenko, et al. Highly accurate protein structure prediction with alphafold. *Nature*, 596(7873):583–589, 2021.

[17] James P Roney and Sergey Ovchinnikov. State-of-the-art estimation of protein model accuracy using alphafold. *Physical Review Letters*, 129(23):238101, 2022.

[18] Minkyung Baek, Frank DiMaio, Ivan Anishchenko, Justas Dauparas, Sergey Ovchinnikov, Gyu Rie Lee, Jue Wang, Qian Cong, Lisa N Kinch, R Dustin Schaeffer, et al. Accurate prediction of protein structures and interactions using a three-track neural network. *Science*, 373(6557):871–876, 2021.

[19] Yufei Huang, Lirong Wu, Haitao Lin, Jiangbin Zheng, Ge Wang, and Stan Z Li. Data-efficient protein 3d geometric pretraining via refinement of diffused protein structure decoy. *arXiv preprint arXiv:2302.10888*, 2023.

[20] Daniel Hesslow, Niccoló Zanichelli, Pascal Notin, Iacopo Poli, and Debora Marks. Rita: a study on scaling up generative protein sequence models. *arXiv preprint arXiv:2205.05789*, 2022.

[21] Lewis Moffat, Shaun M Kandathil, and David T Jones. Design in the dark: Learning deep generative models for de novo protein design. *bioRxiv*, 2022.

[22] Noelia Ferruz, Steffen Schmidt, and Birte Höcker. Protgpt2 is a deep unsupervised language model for protein design. *Nature communications*, 13(1):1–10, 2022.

[23] Erik Nijkamp, Jeffrey Ruffolo, Eli N Weinstein, Nikhil Naik, and Ali Madani. Progen2: exploring the boundaries of protein language models. *arXiv preprint arXiv:2206.13517*, 2022.

[24] Diederik P Kingma and Max Welling. Auto-encoding variational bayes. *arXiv preprint arXiv:1312.6114*, 2013.

[25] Ian Goodfellow, Jean Pouget-Abadie, Mehdi Mirza, Bing Xu, David Warde-Farley, Sherjil Ozair, Aaron Courville, and Yoshua Bengio. Generative adversarial networks. *Communications of the ACM*, 63(11):139–144, 2020.

[26] Jonathan Ho, Ajay Jain, and Pieter Abbeel. Denoising diffusion probabilistic models. *Advances in Neural Information Processing Systems*, 33:6840–6851, 2020.

[27] Yang Song, Jascha Sohl-Dickstein, Diederik P Kingma, Abhishek Kumar, Stefano Ermon, and Ben Poole. Score-based generative modeling through stochastic differential equations. *arXiv preprint arXiv:2011.13456*, 2020.

[28] Namrata Anand and Possu Huang. Generative modeling for protein structures. *Advances in neural information processing systems*, 31, 2018.

[29] Hao Huang, Boulbaba Ben Amor, Xichan Lin, Fan Zhu, and Yi Fang. G-vae, a geometric convolutional vae for proteinstructure generation. *arXiv preprint arXiv:2106.11920*, 2021.

[30] Jason Yim, Brian L Trippe, Valentin De Bortoli, Emile Mathieu, Arnaud Doucet, Regina Barzilay, and Tommi Jaakkola. Se (3) diffusion model with application to protein backbone generation. *arXiv preprint arXiv:2302.02277*, 2023.

[31] Kevin E Wu, Kevin K Yang, Rianne van den Berg, James Y Zou, Alex X Lu, and Ava P Amini. Protein structure generation via folding diffusion. *arXiv preprint arXiv:2209.15611*, 2022.

[32] Brian L Trippe, Jason Yim, Doug Tischer, Tamara Broderick, David Baker, Regina Barzilay, and Tommi Jaakkola. Diffusion probabilistic modeling of protein backbones in 3d for the motif-scaffolding problem. *arXiv preprint arXiv:2206.04119*, 2022.

[33] Zhangyang Gao, Cheng Tan, and Stan Z Li. Pifold: Toward effective and efficient protein inverse folding. *arXiv preprint arXiv:2209.12643*, 2022.

[34] Bowen Jing, Stephan Eismann, Patricia Suriana, Raphael JL Townshend, and Ron Dror. Learning from protein structure with geometric vector perceptrons. *arXiv preprint arXiv:2009.01411*, 2020.

[35] Alexey Strokach, David Becerra, Carles Corbi-Verge, Albert Perez-Riba, and Philip M Kim. Fast and flexible protein design using deep graph neural networks. *Cell systems*, 11(4):402–411, 2020.

[36] Namrata Anand, Raphael Eguchi, Irimpan I Mathews, Carla P Perez, Alexander Derry, Russ B Altman, and Po-Ssu Huang. Protein sequence design with a learned potential. *Nature communications*, 13(1):1–11, 2022.

[37] Shitong Luo, Yufeng Su, Xingang Peng, Sheng Wang, Jian Peng, and Jianzhu Ma. Antigen-specific antibody design and optimization with diffusion-based generative models. *bioRxiv*, pages 2022–07, 2022.

[38] Wengong Jin, Jeremy Wohlwend, Regina Barzilay, and Tommi Jaakkola. Iterative refinement graph neural network for antibody sequence-structure co-design. *arXiv preprint arXiv:2110.04624*, 2021.

[39] Justin Gilmer, Samuel S Schoenholz, Patrick F Riley, Oriol Vinyals, and George E Dahl. Neural message passing for quantum chemistry. In *International conference on machine learning*, pages 1263–1272. PMLR, 2017.

[40] Andrew W Senior, Richard Evans, John Jumper, James Kirkpatrick, Laurent Sifre, Tim Green, Chongli Qin, Augustin Žídek, Alexander WR Nelson, Alex Bridgland, et al. Improved protein structure prediction using potentials from deep learning. *Nature*, 577(7792):706–710, 2020.

[41] Vıctor Garcia Satorras, Emiel Hoogeboom, and Max Welling. E (n) equivariant graph neural networks. In *International conference on machine learning*, pages 9323–9332. PMLR, 2021.

[42] Michael Schaarschmidt, Morgane Riviere, Alex M Ganose, James S Spencer, Alexander L Gaunt, James Kirkpatrick, Simon Axelrod, Peter W Battaglia, and Jonathan Godwin. Learned force fields are ready for ground state catalyst discovery. *arXiv preprint arXiv:2209.12466*, 2022.

[43] Sheheryar Zaidi, Michael Schaarschmidt, James Martens, Hyunjik Kim, Yee Whye Teh, Alvaro Sanchez-Gonzalez, Peter Battaglia, Razvan Pascanu, and Jonathan Godwin. Pre-training via denoising for molecular property prediction. *arXiv preprint arXiv:2206.00133*, 2022.

[44] Marloes Arts, Victor Garcia Satorras, Chin-Wei Huang, Daniel Zuegner, Marco Federici, Cecilia Clementi, Frank Noé, Robert Pinsler, and Rianne van den Berg. Two for one: Diffusion models and force fields for coarse-grained molecular dynamics. *arXiv preprint arXiv:2302.00600*, 2023.

[45] Jonathan Godwin, Michael Schaarschmidt, Alexander Gaunt, Alvaro Sanchez-Gonzalez, Yulia Rubanova, Petar Veličković, James Kirkpatrick, and Peter Battaglia. Simple gnn regularisation for 3d molecular property prediction & beyond. *arXiv preprint arXiv:2106.07971*, 2021.

[46] Zhangyang Gao, Cheng Tan, and Stan Z. Li. Pifold: Toward effective and efficient protein inverse folding. *ArXiv*, abs/2209.12643, 2022.

[47] Zhangyang Gao, Cheng Tan, Stan Li, et al. Alphadesign: A graph protein design method and benchmark on alphafolddb. *arXiv preprint arXiv:2202.01079*, 2022.

[48] Adam Leach, Sebastian M Schmon, Matteo T Degiacomi, and Chris G Willcocks. Denoising diffusion probabilistic models on so (3) for rotational alignment. 2022.

[49] Siegfried Matthies, J. Muller, and G. W. Vinel. On the normal distribution in the orientation space. *Textures and Microstructures*, 10:77–96, 1988.

[50] Dmitry Nikolayev and Tatjana I. Savyolov. Normal distribution on the rotation group so(3). *Textures and Microstructures*, 29:201–233, 1997.

[51] Jean Gallier and Dianna Xu. Computing exponentials of skew-symmetric matrices and logarithms of orthogonal matrices. *International Journal of Robotics and Automation*, 18(1):10–20, 2003.

[52] Ricky TQ Chen, Yulia Rubanova, Jesse Bettencourt, and David K Duvenaud. Neural ordinary differential equations. *Advances in neural information processing systems*, 31, 2018.

[53] Ashish Vaswani, Noam Shazeer, Niki Parmar, Jakob Uszkoreit, Llion Jones, Aidan N Gomez, Łukasz Kaiser, and Illia Polosukhin. Attention is all you need. *Advances in neural information processing systems*, 30, 2017.

[54] Diederik P Kingma and Jimmy Ba. Adam: A method for stochastic optimization. *arXiv preprint arXiv:1412.6980*, 2014.

[55] Cheng Tan, Zhangyang Gao, Jun Xia, and Stan Z Li. Generative de novo protein design with global context. *arXiv preprint arXiv:2204.10673*, 2022.

[56] Baris E Suzek, Yuqi Wang, Hongzhan Huang, Peter B McGarvey, Cathy H Wu, and UniProt Consortium. Uniref clusters: a comprehensive and scalable alternative for improving sequence similarity searches. *Bioinformatics*, 31(6):926–932, 2015.

[57] Zhixiu Li, Yuedong Yang, Eshel Faraggi, Jian Zhan, and Yaoqi Zhou. Direct prediction of profiles of sequences compatible with a protein structure by neural networks with fragment-based local and energy-based nonlocal profiles. *Proteins: Structure, Function, and Bioinformatics*, 82(10):2565–2573, 2014.

[58] Noah Ollikainen and Tanja Kortemme. Computational protein design quantifies structural constraints on amino acid covariation. *PLoS computational biology*, 9(11):e1003313, 2013.

[59] Rhiju Das and David Baker. Macromolecular modeling with rosetta. *Annu. Rev. Biochem.*, 77:363–382, 2008.

[60] Guoli Wang and Roland L Dunbrack Jr. Pisces: a protein sequence culling server. *Bioinformatics*, 19(12):1589–1591, 2003.

[61] Paul J Carter. Potent antibody therapeutics by design. *Nature reviews immunology*, 6(5):343–357, 2006.

[62] Zeming Lin, Halil Akin, Roshan Rao, Brian Hie, Zhongkai Zhu, Wenting Lu, Nikita Smetanin, Robert Verkuil, Ori Kabeli, Yaniv Shmueli, et al. Evolutionary-scale prediction of atomic-level protein structure with a language model. *Science*, 379(6637):1123–1130, 2023.

A Appendix

A.1 Training details

We provide the main hyperparameters of DNDesign in Table 3.

Table 3: DNDesign-PiFold hyperparameters.

	DNDesign-PiFold	DNDesign-PiFold (uniref)
Strutcure encoder layers	2	4
Sequence decoder layers	2	4
Folding physics learning layers	4	4
Transformer embedding dim	128	128
Attention heads	4	4
Top K neighbors	30	30
Batch size (tokens per GPU)	6000	6000
GPUs	1	1
CATH:AF2 mixing ratio	1:0	1:6
Epochs	100	150
Optimizer	Adam	Adam
β_1	0.9	0.9
β_2	0.999	0.999
Learning rate schedule	OneCycleLR	OneCycleLR
Learning rate	1e-3	1e-3
Annealing strategy	Cosine	Cosine
Increasing learningrate steps percent	30%	30%

Table 4: Protein sequence design comparison on TS50, TS500, and Ollikainen. PP and SR indicate perplexity and sequence recovery, respectively.

Model	TS50		TS500		Ollikainen	
	PP	SR	PP	SR	PP	SR
PiFold	3.71±0.08	57.37±1.32	3.38±0.03	59.74±0.11	3.70±0.10	56.95±0.44
DNDesign-PiFold	3.77±0.02	55.58±0.37	3.34±0.01	59.55±0.45	3.68±0.06	57.42±0.32

A.2 Other datasets

To estimate the generalization ability of FFDesign, we extend FFDesign on various real-world datasets, TS50, TS500 [57], and Ollikainen [58] datasets. The first two datasets include randomly selected 50 and 500 non-redundant proteins from PISCES server [60], respectively. Ollikainen dataset has 40 proteins sampled from diverse protein domains to explore structural constraints on amino acid covariation. For a download issue, 37 proteins are used in this work. We evaluate CATH4.2 pre-trained PiFold and DNDesign-PiFold in a zero-shot setting. All results are shown in Table 4. In the case of a TS50 dataset with a small number of 50 proteins, DNDesign performs worse. However, when handling a larger dataset of 500 points in TS500, a gain in perplexity is observed. The Olikainen dataset demonstrates performance gains in both perplexity and sequence recovery.

A.3 Multi-chain sequence design

Designing a specific part of a protein assembly, which is a complex of single proteins, is one of the most common and important problems in protein design, such as the problem of fixing complementarity determining region (CDR) loop in an antigen-antibody complex [61]. To evaluate the performance of the inverse-folding models for these scenarios, we design the task of designing subunit protein sequences of protein assemblies. Following ProteinMPNN [9], we train models using protein assemblies from PDB [10]. In training, models are tasked to generate amino acids of a target chain when given a whole protein complex. For evaluation, we select 178 protein assemblies containing more than four protein chains from the test set, and conduct sequence design on multiple chains in alphabetical chain order. As shown in Table 5, DNDesign gives marginal gains.

Table 5: Comparison of FFDesign with previous models on multimer sequence design of protein heteromer assemblies. All results are newly calculated.

Model	1	2	3	4	Avg
PiFold	46.75	46.75	46.75	46.75	46.75
DNDesign-PiFold	46.70	46.90	46.94	46.74	46.82

A.4 Inference speed

We compared the inference time on the same machine (single V100) for all proteins in CATH4.3 test set. As shown in Table 6, there is no significant inference time difference compared to the previous methods. While DNDesign-PiFold performs better than ESM-IF (53.75% vs 51.60%) and have several times less parameters (5M vs 140M), DNDesign-PiFold has twice the faster inference rate.

Table 6: Inference speed on CATH 4.3 test set.

Model Type	Time(min)
ProteinMPNN	19
PiFold	20
DNDesign-PiFold	22
ESM-IF	67

A.5 Ablation study

In order to understand the effectiveness of each proposed operation, we conduct an ablation study as shown in Table 7. All models are trained in the same setting for CATH 4.2 benchmark. Without

Table 7: Ablation of five components of DNDesign.

	Perplexity ↓	Recovery % ↑
Baseline	4.70	48.06
ForceInit	4.62 (-0.08)	48.52 (+0.46)
ForceNode	4.64 (-0.06)	48.76 (+0.70)
ForceEdge	4.58 (-0.12)	49.33 (+1.27)
GlobalForce	4.65 (-0.05)	48.51 (+0.45)
ForceLogits	4.64 (-0.06)	48.76 (+0.70)
ForceInit + ForceNode	4.52 (-0.18)	49.66 (+1.60)
ForceInit + ForceNode + ForceEdge	4.52 (-0.18)	49.52 (+1.46)
ForceInit + ForceNode + ForceEdge + GlobalForce	4.52 (-0.18)	50.00 (+1.94)
ForceInit + ForceNode + ForceEdge + GlobalForce + ForceLogits	**4.46** (-0.24)	**50.00** (+1.94)

Table 8: Comparison of sequence recovery on CATH 4.2 with regard to structrual environment: core and surface. We categorize residues by density of neighboring C_α atoms within 10 angstroms of the central residue C_α atom. Core and surface residues have more than 24 and less than 16 neighbors, respectively.

Model	Recovery % ↑	
	Core	Surface
PiFold	66.67	40.00
DNDesign-PiFold	**66.67**	**40.74**

our proposed operations, the baseline model shows 4.70 and 48.06% of perplexity and recovery, respectively. The best effective module is ForceEdge, which boosts improvements of -0.12 and 1.27% over the baseline. Also, ForceInit and ForceNode modules benefit models on both perplexity and recovery by -0.08, -0.06, and 0.46%, 0.70%, respectively. Other operations also show performance gains over baselines. All results confirm that our proposed operations effectively transfer learned folding physics knowledge to the entire networks.

Table 9: Comparison of sequence recovery on CATH 4.3 with regard to structrual environment: core and surface.

Model	Recovery % ↑	
	Core	Surface
ESM-IF	39.00	72.00
DNDesign-PiFold (scaled-up)	**43.48**	**75.00**

Recovery depending on the structural context Table 8 shows the sequence recovery performance of PiFold and DNDesign-PiFold on the core and surface residues of test proteins in the CATH4.2. We observe that both models perform better in core residue design than the surface. The results are in line with [8]. Also, we see that DNDesign-PiFold benefits on surface scenario. This is meaningful in terms of applications because many protein applications, such as enzymes and antibody-antigens, occur on surface residues rather than core residues. Also, Table 9 reveal that DNDesign-PiFold effectively generate sequences in core and surface compared to ESM-IF, which has several times larger parameters compared to DNDesign-PiFold.

Force logit ratio ablation study In order to confirm the inverse folding performance according to the force logits during training and inference, we train DNDesign-PiFold on CATH4.2 by varying the ratio (0.2, 0.4, 0.6, 0.8) during training. As shown in Table 10, all models have same sequence recovery performance, meaning that mixing force logits to inverse-folding logits benefits with any ratio. Also, the model with 0.2 force ratio shows the best performance. In addition to this, we ablate the force ratio during inference using a model trained with 0.2 force logits ratio during training. As shown in Table 11, 0.2 ratio gives best performance. WIth the empirical results, we use force logit ratio of 0.2 for both training and inference.

A.6 Limitations

Inverse-folding, a powerful method that enables fine-grained protein engineering when a known structure exists, has been used in various protein engineering. Therefore, it has a limitation that it can be performed only when a known structure exists. Fortunately, the limitation is somewhat

Table 10: Hyper-parameter search of force logit ratio during training.

Ratio	0.2	0.4	0.6	0.8
Perplexity	4.46	4.47	4.51	4.50
Sequence recovery	50.0	50.0	50.0	50.0

Table 11: Hyper-parameter search of force logit ratio during inference.

Ratio	0.0	0.1	0.2	0.3	0.4	0.5	0.6	0.7	0.8
Perplexity	4.58	4.48	4.46	4.56	4.84	5.38	6.32	7.87	10.33

alleviated because models like AlphaFold2 [16], RoseTTAFold [18], and ESMFold [62] correctly predict structures of proteins that have not yet been experimentally characterized. However, there are proteins that these models fail, such as orphan proteins and antibody-antigen complexes, because the proteins lacks multiple sequence alignments that is key inputs for those models. Additionally, the requirement that the structures in the dataset need to be locally optimized (with low energy) is the bottleneck for FFDesign training. We think that numerous samples in the predicted structures do not meet the requirement. So, we suspect that these structures may negatively impact the learning of the local minimized structure distribution if included in the training dataset. However, we believe that the two constraints brought by the aforementioned structure dependency can be resolved with better structure prediction. Meanwhile, recently, Dauparas et al [9] has experimentally verified in web-lab that protein design is possible more successfully than previously widely used computational methods by combining an inverse-folding model with a structure generation model. In conclusion, even though inverse-folding has structural dependencies, the design method is still a powerful strategy for designing multiple proteins that match the target fixed structure.

A.7 Broader impact

Proteins are a promising material used in numerous fields, such as drug development, enzymes, and carbon capture. Therefore, designing proteins that meet specific objectives is crucial but challenging because even a single amino acid change can lead to significant property changes. However, one structure can have numerous sequence combinations of 20 amino acids. Optimizing and narrowing candidates ultimately allows us to save considerable human and material resources required for extensive experiments in candidate screening through wet-lab experiments, which leads to significant environmental and economic benefits. We expect that our approach is a promising solution to gain the mentioned advantages.